Sensors and Materials, Vol. 14, No. 4 (2002) 209–218
MYU Tokyo

S & M 0483

A Multifunctional Sensor-Chip based on Micromachined Chamber Array

Jianzhong Zhu, Ziqiang Zhu, Zongsheng Lai, Rong Wang[1], Xiaqin Wu
Guoxiong Zhang[1] and Zongrang Zhang[1]

IT College, East China Normal University, Shanghai 200062, China
[1]Shanghai Teachers University, Shanghai 2000234, China

(Received June 21, 2001; accepted January 4, 2002)

Key words: biosensor, potassium ion-selective-electrode, micromachining technology, chitosan membrane

This paper reports the fabrication and characterization of a sensor-chip based on a 2×2 microchamber array produced on silicon by anisotropic etching. The chip consists of a glucose sensor, a glutamate sensor, a galactose sensor and a potassium ion-selective-electrode. The structure of the microchamber-array has improved membrane adhesion and mechanical stability and can offer the place-selective immobilization of the enzymes. A chitosan membrane is used not only to immobilize the enzyme on the working electrode but also to prevent the penetration of interferents such as uric and ascorbic acids. The fabricated chips have shown attractive performances such as high sensitivity and good stability.

1. Introduction

The need for microbiosensors and ion-selective microelectrodes in medicine, food and processing-technologies has increased dramatically in the last decade. A wide variety of enzyme-based biosensors have already been developed. Yet the detection of glucose in human blood is the most widespread and important application of biosensors. Standard planar processes and micromachining technology offer the possibility of mass-production of glucose microsensors.[1–4] However, to date, most enzymatic microsensors involved a membrane fixed on top of the transducer, which leads to malfunctioning of the sensor due to inadequate adhesion and poor mechanical stability of the membrane. Dip-coating procedures were not sufficiently reproducible to obtain sensors with identical performance. Sensors with membranes that were separately cast and mounted onto an electrode

are not easy to miniaturize and are therefore not suitable for potential implantation. Furthermore, place-selective immobilization of the membrane material, which is a precondition for the development of multi-functional sensors, is difficult to achieve. To overcome these problems, a novel device structure was designed by Steinkuhl *et al.*[5] Enzyme membrane is deposited in pyramidal containment produced on silicon by anisotropic etching. In the present study, a chip with glucose, glutamate, galactose enzymes sensor and potassium ion-selective-electrode (K^+ISE) on the basis of the microchamber array have been successfully fabricated and their performances were characterized. Compared with the previous structure, several significant modifications have been made. 1) A single containment was extended to a 2×2 chamber array in a chip, which makes it possible to fabricate 4-functional sensors. 2) A working electrode (WE) of Pt and a reference electrode (RE) of Ag/AgCl were integrated on a chip to improve the reliability and stability of the sensors and it is more convenient in practical use.

On the other hand, the elimination of interference is required for practical application of biosensors, although intensive research activities have been devoted to the problem.[6–8] A number of studies on amperometric biosensors have shown the use of a diffusion limit membrane (acetylcellulose, Nafion™, etc.) can prevent interference species such as ascorbic acid, uric acid and acetaminophen in biological fluid samples.[9–12] In the present work, a double-functional chitosan membrane was first introduced to immobilize the enzyme on the WE and to prevent the penetration of interferents such as uric and ascorbic acids, as well.

2. Experimental

2.1 *Chemicals*

All reagents were of analytic grade. Glucose oxidase (GOD, EC. 1.1.3.4, 23800 u/g, from Aspergillus niger), galactose oxidase (GalOD, EC. 1.1.1.9, from Dactylium dendroides, 3000 u/g), glutamate oxidase (GluOD, EC. 1.4.3.11, from Streptomyces sp. 5 u/mg), chitosan, glutaraldehyde (Grade II 25% aqueous solution), valinomycin, dioctyl phthalate, and tetrahydrofurun were used as received from Sigma.

2.2 *Microchip preparation*

A schematic of a designed microchip is shown in Fig. 1. A 2-inch Pyrex glass sheet with 0.8–1.0 mm thickness is used for the down-substrate as the carrier of the WE. A 50 nm titanium intermediate layer and a 200 nm platinum layer were successively formed on the down-substrate after standard cleaning procedures by electron beam evaporation. The titanium layer acted as an adhesion layer. The lift-off technique was used for patterning 1.0 ×1.0 mm^2 of Pt WEs, 0.2×1.5 mm^2 of conduction lines and 0.5×0.5 mm^2 of pads. A piece of a 2-inch size and 0.38-mm-thick p-type silicon (100) wafer covered with a 1.5-μm-thick SiO_2 layer was used as the up-substrate. Quadratic holes (1.2×1.2 mm^2) on the SiO_2 layer were formed by photolithgraphic and etching processes. After the removal of photoresist and protective layers on the back, silicon was etched anisotropically in 40% KOH solution at 50°C for 10 h to create the four pyramidal cavities. Four channels with 1 μm depth and 0.3 mm width were also etched on the surface located at the WE conducting lines. The

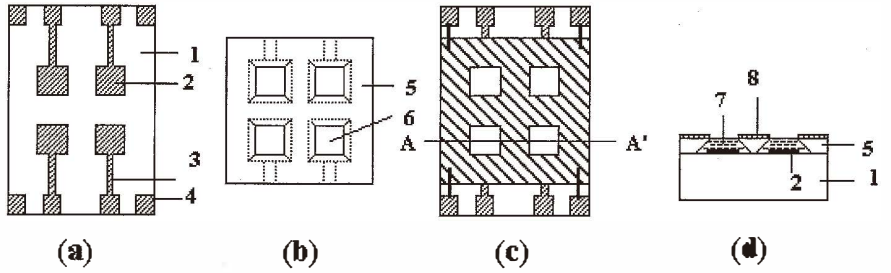

Fig. 1. A schematic of designed microchip. 1. Pyrex glass down-substrate, 2. Pt WE, 3. Conduction line, 4. Pads, 5. Up-substrate made of silicon, 6. Quadratic hole, 7. chitosan membrane with cross-linked enzyme, 8. Ag/AgCl RE. (a) Down-substrate, (b) up-substrate, (c) bonding between up- and down-substrates, (d) cross section along A-A'.

SiO_2 thin layer was removed by etching with hydrofluoric acid and then the wafer was oxidized to form a 0.1–0.2-μm-thick SiO_2 layer over the whole surface. A 400-nm-thick silver layer was evaporated on the back of the up-substrate. Partial chlorination of the silver layer was performed in 0.25 mol/L $FeCl_3$ solution to form the Ag/AgCl RE onto the back. After chip separation, anode bonding between up- and down-substrates was carried out under a bias of 300 V for each chip at 500°C for several minutes. The microchip of 7×5 mm^2 was mounted on a printed circuit board (PCB), followed by wire bonding. An epoxy resin was used to encapsulate the sensor, leaving the active area exposed.

2.3 *Immobilization*

1 g of chitosan was added into 4 ml of acetic acid and stirred for 20 min until complete dissolution. One microliter of chitosan solution was transferred into each microchamber of the arrays and naturally dried. Then it was rinsed several times with deionized water to remove residual acetic acid in the chitosan membrane and dried. Next it was immersed into 2.5% glutaradehyde solution for 5 min. One microliter of 1000 U/ml GOD, GluOD and GalOD were respectively transferred into three microchambers of the array. After drying, they were rinsed several times with deionized water to remove the unimmobilized enzyme, followed by natural drying before being used.

2.4 *Preparation of K^+ISE*

One mg of valinomycin was added into 50 mg dioctyl phthalate (plasticizer) followed by a mixture of 700 mg tetrahydrofuran solution containing 3% (w/w) PVC resin powder. Ten microliters of the mixture solution was added into the 4^{th} chamber of the array to form a potassium-sensing PVC membrane on the Pt WE surface.

2.5 *Measurement*

The PCB was connected to a CHI 600 A Electrochemical Analyzer and a Digit Ionometer (China) throughout a ribbon connector with 4-channel of witch. All electrochemical measurements were performed in the two-electrode mode. For biosensor testing the applied working potential was set to +700 mV versus the Ag/AgCl RE.

3. Results and Discussions

3.1 *Semipermeability of the chitosan membrane*

Chitosan is a natural high biopolymer and a product of deacetylation of chitin. It can been dissolved into dilute acid. The molecular structure of chitosan is similar to that of cellulose; the only difference is an amine is present for chitosan and a hydroxyl group for cellulose in the C-2 position, as shown in Fig. 2. The cross-link reaction can occur between chitosan and enzyme due to the presence of free amine in the molecular structure of chitosan. Cellulose acetate membrane was observed to be permeable for hydrogen peroxide but impermeable for interference species.[10-12] Thus, a chitosan membrane has double function, i.e. to immobilize enzyme on the WE and to prevent the penetration of interferents such as uric and ascorbic acids.

Figures 3–6 show the cyclic voltammograms with a scan rate of 50 mV/s between the bare electrode (a) and the electrode with the chitosan membrane (b) in four different solutions: $K_3Fe(CN)_6$, H_2O_2, uric and ascorbic acids, respectively. The response current for

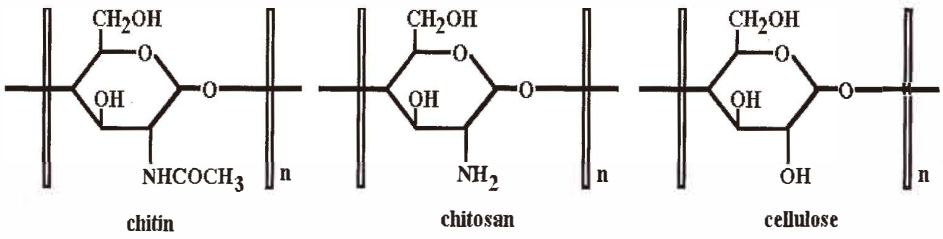

Fig. 2. The molecular structures of chitin, chitosan and cellulose.

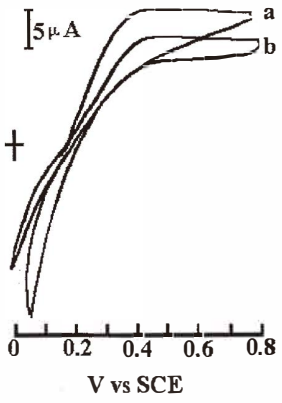

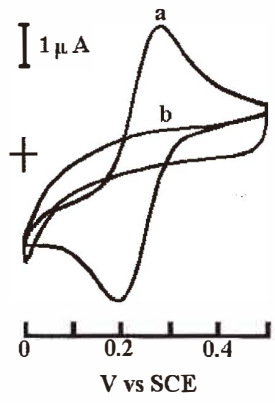

Fig. 3 (left). The cyclic voltammograms in H_2O_2 solution for the electrodes (a) without and (b) with the chitosan membrane.

Fig. 4 (right). The cyclic voltammograms in $K_3Fe(CN)_6$ solution for the electrodes (a) without and (b) with the chitosan membrane.

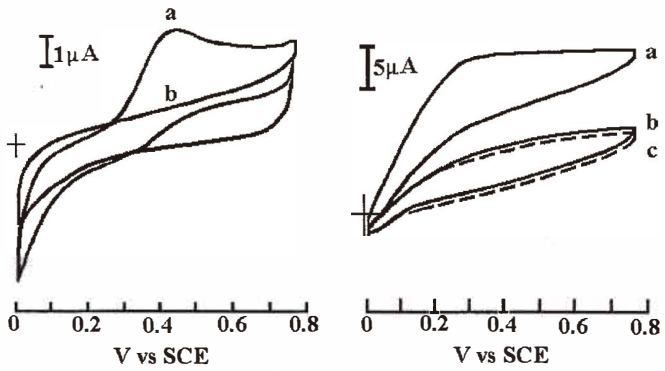

Fig. 5 (left). The cyclic voltammograms in uric acid solution for the electrodes (a) without and (b) with the chitosan membrane.
Fig. 6 (right). The cyclic voltammograms in ascorbic acid solution for the electrodes (a) without and (b) with the chitosan membrane, (c) the electrodes without the chitosan membrane in bulk solution (dotted line).

the electrode with the chitosan membrane decreases by 20% in H_2O_2 solution and almost to the bulk current in the ascorbic acid solution. The oxide peaks of $K_3Fe(CN)_6$ and uric acid disappear in the case of the electrodes with the chitosan membrane. It is obvious that the chitosan membrane is permeable for H_2O_2 but impermeable for larger molecules such as $K_3Fe(CN)_6$ uric and ascorbic acids. Hence, the chitosan membrane can play an important role in resistance to interference.

3.2 *Respose time*

The response times of the glucose sensor were 20 s for concentration change from 0 to 6 mmol/L and 30 s for reversion. They were estimated from the response-time curve using a potentiostat set at +700 mV (Fig. 7) indicating the establishment of stable mass transport within 30 s. Response times for other sensors were also within 30 s.

3.3 *Calibration curves*

The calibration curves of the glucose sensor, glutamate sensor and galactose sensor are shown in Fig. 8. Linear ranges were 0.1–10.0 mmol/L for the glucose sensor, 0.1–10.0 mmol/L for the glutamate sensor and 0.1–6.0 mmol/L for galactose sensor. Figure 9 shows the calibration curve for the K^+ISE. The linear range was 1.0×10^{-4} – 0.1 mol/L and its slope is 57.0 mV/decade, near the theoretical value of 59.1 mV/decade.

3.4 *Precision*

Good precision was confirmed by 10 continuous measurements in pH 6.86 phosphate buffer solutions containing 4 mmol/L glucose, glutamate and galatose. The experimental values are listed in Table 1.

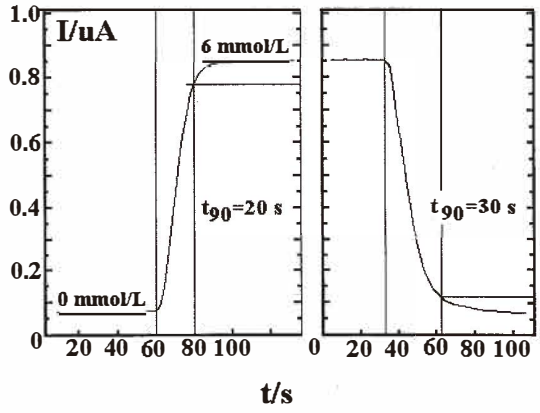

Fig. 7. Response-time curve for the glucose sensor.

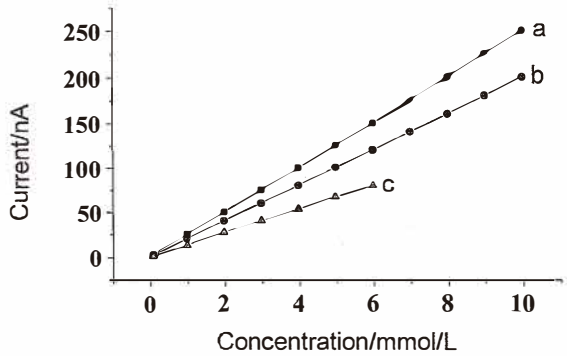

Fig. 8. Typical calibration curves for the (a) glucose sensor, (b) glutamate sensor and (c) galactose sensor.

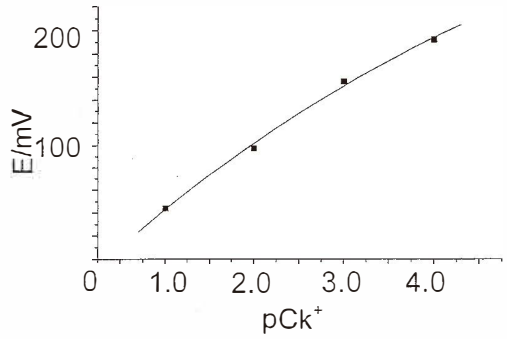

Fig. 9. Typical calibration curve for the K^+ISE.

Table 1
Precision of the biosensors.

Measurement times	Glucose (nA)	Glutamate (nA)	Galactose (nA)
1	99	76	54
2	103	74	53
3	98	77	51
4	101	78	52
5	101	75	53
6	100	74	55
7	102	76	53
8	103	76	54
9	100	77	52
10	101	78	55
Average value	101	76	53
RSD	1.6%	2.1%	2.5%

RSD: Relative standard deviation

3.5 *Long-term stability*

The long-term stability of the chip is shown in Fig. 10. The decrease in response current of the enzyme sensor was observed during the first several days. This may be due to the loss of unimmobilized enzymes. However, no apparent changes in the current were observed during the following 65 days for the glucose sensor, 30 days for the glutamate sensor, 20 days for galactose sensor, and 70 days after the preparation of chip for K^+ISE. The GalOD easily lost its activity without protection of Cu^{2+}.[13] Hence, several microliters of 0.4 mmol/L $CuSO_4$ solution was dropped into the microchamber of the galactose sensor in order to protect the activity of the GalOD for storage.

3.6 *Interference and cross-talk effect*

For practical application, it is necessary to clarify the effects of the interference of coexisting components on response current and the cross-talk effect between the sensors. As an example, the response current of the glucose sensor was compared between the glucose standard solution with and without coexisting components. The total quantities of the coexisting components were 4.0, 131.6, 96.8, 2.66, 6.83, 1.0, 0.132, 0.392 and 0.057 mmol/L for K^+, Na^+, Cl^-, Ca^{2+}, urea, galatose, creatinine, uric and ascorbic acids, respectively, similar to the concentration in normal human blood serum. The difference between the standard value of 6.0 mmol/L and the measured value of 5.9 mmol/L is within the acceptable range of experimental error. In the range of the above quantities, therefore, no significant interference or cross-talk effect was observed. The interference for other sensors is similar to that for the glucose sensor.

3.7 *Accuracy*

Measurements of accuracy of the sensors were taken with the glucose sensor, galactose sensor and K^+ISE in a standard serum with composition similar to that of normal human blood serum. The measured values of glucose, galactose and K^+ were 6.1, 1.0 and 4.0 mmol/L, which are almost identical to the recommended values of 6.0, 1.1 and 4.1 mmol/L, respectively.

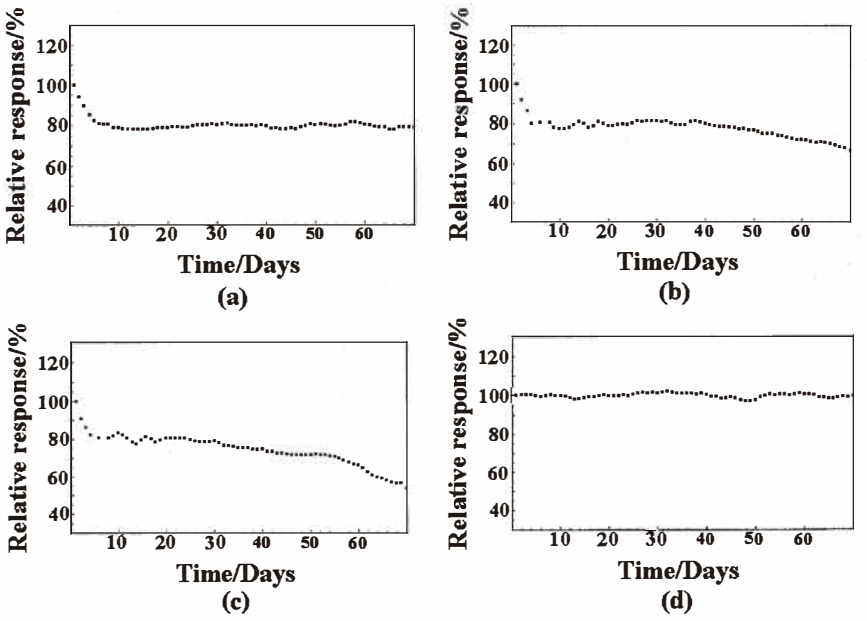

Fig. 10. Long-term stability of (a) glucose sensor, (b) glutamate sensor, (c) galactose sensor and (d) K^+ISE. Sensor response for 4 mmol/L-substrate was measured 10 times a day. The average value for 10 measurements is plotted against days after the preparation of the chip.

Results obtained from the glucose sensor, galactose sensor and K^+ISE directly in human blood serum were compared with those obtained by spectrophotometry or the ion selective electrode method, as shown in Fig.11. On testing 100 samples of serum, the correlation coefficients reach 0.998, 0.996 and 0.996, respectively.

Good accuracy was also confirmed through the measurement of fermented solution diluted 50 times, using the glutamate sensor and spectrophotometry. The measured values are listed in Table 2.

3.8 *Discussions*

Integration of glucose and lactate sensor elements on a chip was reported by Perdomo *et al.*[14], while the integration of four sensors on a chip was performed in the present work. Table 3 gives the performances of glucose sensor elements reported by Perdomo *et al.*[14] and those of our study.

Scheipers *et al.*[15] reported multianalyte sensors with two or three containment sensor elements integrated on a chip. For comparison of K^+ISE sensor elements, Table 4 gives the performance of the K^+ISE sensor element reported by Scheipers *et al.* and that of our study.

A significant improvement of sensitivity and long-term stability is obtained in our sensors, as shown in Tables 3 and 4. The good performance can be attributed to the use of double functional chitosan membrane and the integration of RE on the structure of a 2×2 microchamber array rather than a separate structure in the sensors.

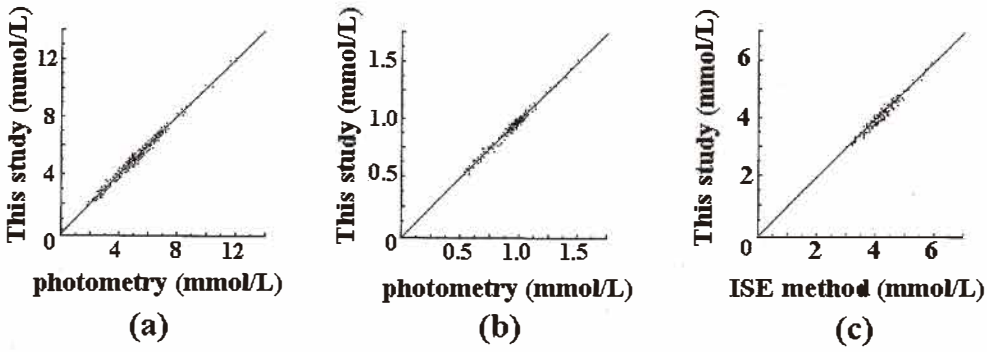

Fig. 11. Correlation and regression line for measurements of 100 human serum samples between spectrophotometry or ion-selective-electrode method and our sensors of (a) glucose, (b) galactose and (c) potassium ion.

Table 2
Accuracy of the glutamate sensor.

Times	1	2	3	4	5	6	7	8	9	10
Results	2.8	2.6	2.3	2.5	2.8	2.5	2.4	2.5	2.2	2.4
AV				2.5 ± 0.2 mmol/L						
RV				2.3 ± 0.1 mmol/L						
Error				0.2 mmol/L						

AV: Average value, RV: Reference value measured by spectrophotometry.

Table 3
Performance of glucose sensor elements.

	Sensitivity nA/(mmol/L)	Linear range mmol	Response time ($T_{90\%}$) s	Long-term stability day
Ref. 14	1.7	0–30	52	–
	3.5	0–10	48	–
	5.6	0–6	35	–
	12.5	0–3	32	–
This study	25	0–10	30	65

Table 4
Performance of K^+ISE sensor element.

	Sensitivity mV/decade	Linear range mmol/L	Long-term stability day
Ref. 15	56.2	—	>30
This study	57	10^{-4}–10^{-1}	>70

4. Conclusions

Glucose sensor, glutamate sensor, galactose sensor and K^+SIE based on a pyramidal microchamber array have been fabricated. The array was produced on a single silicon wafer by the anisotropic etching technique. The performance of sensors has been characterized in terms of cyclic voltammetry and the potentiostat method. They exhibited good response behaviors, particularly stability and repeatability. These have been attributed to the improved membrane adhesion and mechanical stability of the membrane due to the structure of pyramidal chambers.

It is found that the chitosan membrane exhibited good selective permeability, which prevents the penetration of interferents of uric and ascorbic acids during the detection of glucose, glutamate and galactose.

The microchamber-array has shown to have place-selective immobilization of the enzymes, which could lead to the mass-production of multifunctional biosensors.

Acknowledgment

The authors are grateful for the financial support from NSFC (No. 69876044 and No. 69925409), the Shanghai Development Fund of Science and Technology (No. 015211066), the Education Commission of Shanghai Municipal Government and the Key Laboratories of Transducer Technology, Chinese Academy of Sciences.

References

1 E. Mamm-Buxbaum, F. Pittner and T. Schalkhammer: Sensors and Actuators, B**1** (1990) 518.
2 M. Koudelka, F. Rohner-Jeanrenaud, J. Terrettaz, E. Bobbioni-Harsch, N. F. De Rooij and B. Jeanrenaud: Biosensors and Bioelectronics **6** (1991) 31.
3 G. Urban, G. Jobst, F. Kohl, A. Jachimowicz, F. Olcaytug, O. Tilado, P. Goiser, G. Nauer, F. Pittner, T. Schalkhammer and Mann-Buxbaum: Biosensors and Bioelectronics **6** (1991) 555.
4 J. Z. Zhu, J. L. Wu, C. Y. Tian, W. Wu, H. W. Zhang, D. R. Lu and G. X. Zhang: Sensors and Actuators, B**20** (1994) 17.
5 R. Steinkuhl, C. Dumschat, C. Sundermeier, H. Hinkers, R. Renneberg, K. Cammann and M. Knol: Biosensors and Bioelectronics **11** (1996) 187.
6 N. C. Bacon and E. A. H. Hall: Electroanalysis **11** (1999) 749.
7 Q. S. Li: Anal. Lett. **31** (1998) 937.
8 F. Mizutani, Y. Sato, Y. Hirata, T. Sawaguchi and S. Yabuki: Anal. Chim. Acta **364** (1998) 173.
9 S. V. Sasso, R. J. Pierce, R. Walla and A. M. Yacynych: Anal. Chem. **62** (1990) 1111.
10 R. Vaidya and E. Wilkins: Electroanalysis **6** (1994) 677.
11 R. Vaidya, P. Atanasov and E. Wilkins: Med. Eng. Phys. **17**(1995) 416.
12 K. McAteer and R. D. O'Neill: Analyst **121** (1996) 773.
13 F. A. Vega, C. G. Nunez, B. Weigel, B. Hitzmann and J. C. D. Ricci: Anal. Chim. Acta **373** (1998) 57.
14 J. Perdomo, C. Sundermeier, H. Hinkers, O. M. Morell, W. Seifert and M. Knoll: Biosensors and Bioelectronics **14** (1999) 27.
15 A. Scheipers, O. Wabmus, C. Sundermeier, J. Eshold, Th. Weib, M. Gitter, B. Rob and M. Knoll: Anal. Chim. Acta **439** (2001) 29.